Rare Metal Materials and Engineering
Volume 50, Issue 7, July 2021
Available online at www.rmme.ac.cn

Science Press

Cite this article as: Shao Huiping, Yu Xinding, Zhang Yumeng, et al. Preparation of Porous TCP Scaffolds for Cancellous Bone Engineering by 3D Gel-Printing[J]. Rare Metal Materials and Engineering, 2021, 50(07): 2308-2314.

ARTICLE

Preparation of Porous TCP Scaffolds for Cancellous Bone Engineering by 3D Gel-Printing

Shao Huiping[1], Yu Xinding[1], Zhang Yumeng[1], Yang Siming[2]

[1] Institute for Advanced Materials and Technology, University of Science and Technology Beijing, Beijing 100083, China; [2] Key Laboratory of Wound Repair and Regeneration of PLA, Medical College of PLA, Chinese PLA General Hospital, Beijing 100853, China

Abstract: High-strength and high-porosity tricalcium phosphate (TCP) scaffolds were prepared by 3D gel-printing (3DGP) technique. The microstructure of the scaffolds was observed by scanning electron microscopy (SEM) and the biocompatibility was evaluated by animal experiments. The results show that the optimal concentration of solid loading of slurry for printing is 34vol%, and the shrinkage of printing scaffolds along length, width, and height directions is 11.44%±0.20%, 9.41%±0.23%, and 10.57%±0.20%, respectively. After the scaffolds are sintered at 1150 °C for 2 h, the compressive strength of the scaffolds is 22.6±0.12 MPa and the porosity is ~62.1%. The animal implantation experiment shows that the porous TCP scaffolds do not cause significant tissue rejection in rabbit femoral condylar defects, and there is no inflammatory reaction or chronic inflammatory reaction at the bone-to-scaffold junction. In conclusion, the porous TCP scaffolds prepared by 3DGP technique have good biocompatibility and excellent strength properties, which are expected to meet the implantation requirements of cancellous bone.

Key words: TCP; porous scaffolds; 3DGP; rabbit; cancellous bone

Bone defects due to trauma, infection or tumor are a hot topic in bone tissue engineering research[1]. The traditional treatment methods mainly include autologous and allogeneic bone transplantations, but the source of autologous bone is restricted, and the allogeneic bone transplantation may cause immune rejection[2,3]. In order to solve these problems, artificial bone transplantation has received extensive attention from researchers. Bone with hierarchical structure is a multiphase composite composed of organic and inorganic components, including the collagen-mineral composites at sub-nanoscale, and the cortical and cancellous bone at macroscale[4]. The inner portion of cancellous bone has a sponge shape, but the outer layer of cortical bone is very dense[5]. As a natural bone material, cancellous bone has good biocompatibility and hydrophilicity, which is usually used for tissue engineering repair. Due to the poor pressure resistance of allogeneic cancellous bone, the cell proliferation improves and phenotypic stability is maintained[6,7]. Therefore, the bone graft materials with sufficient mechanical strength, biocompatibility, and biodegradability provide a new tool for treating patients with bone defects. Calcium phosphate is a representative of bioceramics, which has been widely concerned by researchers. The applicability of hydroxyapatite (HA) as a bone graft material has been evaluated, but the degradation rate of HA in vivo is very slow[8,9]. Tricalcium phosphate (TCP), which is similar to the inorganic component in human bone tissue[10], has good biocompatibility and osteoinduction[11]. Shao et al[12] found that TCP scaffolds have good biodegradability in simulated body fluid (SBF). Zhang et al[13] reported that the degradation rate of TCP scaffold can be controlled by changing its porous structure. Sun et al[14] prepared a 3D printing degradable calcium phosphate scaffold with antibacterial function, which can be used for mandible regeneration.

Traditional manufacturing methods of porous stents mainly include foaming, adding pore-forming agent, and organic foam impregnation methods. 3D printing has great advantages for preparation of porous bone scaffolds which can meet the requirements of cancellous bone strength, ensure the proper porosity and maintain the physical space required for bone

Received date: July 07, 2020
Foundation item: Key Research and Development Projects of the People's Liberation Army (BWS17J036)
Corresponding author: Yang Siming, Ph. D., Key Laboratory of Wound Repair and Regeneration of PLA, Medical College of PLA, Chinese PLA General Hospital, Beijing 100853, P. R. China, E-mail: ysm0117@126.com

regeneration[15]. Recently, 3D printing has the potential to print individualized scaffolds with precise shapes and sizes[16,17]. The 3D image of the bone defect site is obtained by computer-aided drawing, and then the personalized 3D scaffold can be obtained[18-21].

3D gel printing (3DGP)[22] has the advantages of low cost and high efficiency, which has been used to prepare porous ceramic scaffolds, such as HA[8] and $CaSiO_3$ scaffolds[1]. In this study, pure TCP scaffolds were prepared by 3DGP and initially implanted into the bone defect site of rabbits. The rheological properties of printing slurry, and the appearance, compressive strength and the porosity of green and sintered scaffolds were studied. In addition, the biocompatibility of the scaffolds in rabbits was also studied. The porous scaffolds are expected to be used in cancellous bone repairing materials.

1 Experiment

TCP (AR, Shandong West Asia Chemical Co., Ltd), acrylamide monomer (AR, Tianjin GuangFu Fine Chemicals), N, N′-methylenebisacrylamide (AR, Sinopharm Chemical Reagent Co., Ltd), ammonium citrate (AR, Beijing Yili Fine Chemicals) and polyvinyl alcohol (PVA, AR, Jiangxi Alpha Gaoke Pharmaceutical Co., Ltd) were used in this study.

Different materials of 1.20 g acrylamide, 0.2 g ammonium citrate, 0.1 g PVA and 0.1 g N, N′-methylenebisacrylamide were added into the deionized water. Then TCP powders and dispersant (citric acid) were slowly added into the solution to obtain the slurry. By adjusting the dispersant content and solid loading, the viscosity of the slurry was determined.

Fig. 1 shows the schematic diagram for preparing porous TCP scaffolds by 3DGP technique[23]. Firstly, the 3D model was drawn by 3D modeling software (Proe) and exported to stereolithography (STL) file. Secondly, STL file was imported into the slicing software, and then the output data was obtained by G-code after adjusting appropriate print parameters. Then the prepared slurry was transferred to the barrel of the laboratory-made printer, the air pressure was adjusted to make the slurry extrude smoothly, and the scaffold was printed layer by layer. Finally, the printed green scaffolds were solidified at room temperature and sintered.

Fig. 2 shows thermogravimetric (TG) curve of porous TCP green scaffolds. Firstly, the temperature was slowly raised to 150 °C for 3 h to evaporate the water, and then raised to 450 °C for 3 h to remove the polyvinyl alcohol. As shown in Fig. 2, the organic matter in the green scaffolds completely decomposed at 600 °C. After the temperature was raised to 1150 °C for 2 h, the porous TCP scaffolds with excellent performance was obtained.

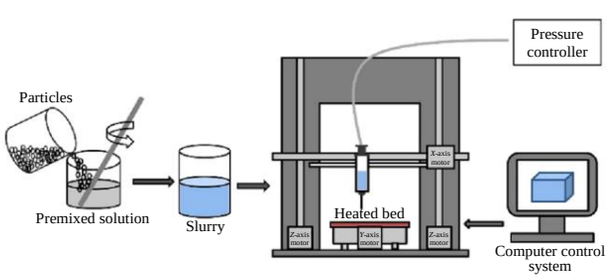

Fig.1 Schematic diagram for preparing porous TCP scaffolds by 3DGP technique[23]

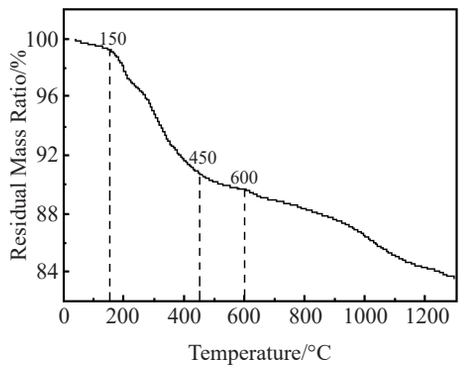

Fig.2 TG curve of TCP green scaffolds with heating rate of 10 °C/min

The total porosity (P) of the scaffolds was measured by drainage method[24-26]. The surface morphology of porous scaffolds was observed by scanning electron microscope (SEM). The compressive strength of the scaffolds was measured by a universal test machine (WDW-200D). Five TCP scaffolds were used to measure the shrinkage of porous scaffolds in all directions.

A bone defect of 3 mm in diameter and 3 mm in height was made in the right forelimb of New Zealand white rabbit, and the printed scaffolds were implanted into the defect site. X-ray examination of the rabbit right forelimb was performed at 1, 3, and 6 weeks after the surgery. The purpose was to observe the repairing status of bone defects in rabbits at different time periods. Fig. 3 shows the bone defect at femoral condyle before and after implantation of porous scaffold.

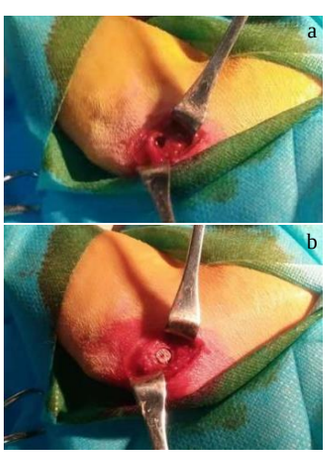

Fig.3 Bone defect at femoral condyle before (a) and after (b) implantation of porous scaffold

2 Results and Discussion

2.1 Characteristic analysis of powders

Fig.4a shows the morphology of TCP powders. These powders have a nearly spherical morphology with good overall dispersion and no obvious agglomeration is found. Fig. 4b shows the average size of TCP powders is about 8.99 μm. When the particle particle size is small, the surface activation energy is large, the microstructure becomes dense, and the mechanical properties improve after sintering. Besides, the small size of particle is beneficial to the degradation of scaffolds.

2.2 Rheological properties of slurry

The viscosity, solid loading and stability of the printing slurry are important for the preparation of high performance porous TCP scaffolds. As shown in Fig.5a, the slurry viscosity decreases and then increases when the dispersant content in the slurry increases. When the dispersant content in the slurry is less than 0.5wt%, the raw material powder cannot be uniformly dispersed, and the slurry has poor fluidity, which cannot meet the requirements of extrusion molding. When the dispersant content is 3.0wt%, the slurry viscosity is larger, and thereby a large pressure for material extrusion is required. When the dispersant content is between 1.5wt%~2.5wt%, the printing line is uniform and there is no broken line. At the same time, the extrusion is stable and continuous, and the nozzle is not clogged. When the dispersant content is 1.0wt%, the viscosity of the slurry is the lowest. However, the nozzle clogging and water droplets often occur during the printing process, indicating that the slurry is not sufficiently dispersed. Therefore, the optimal dispersant content is 2.0wt% in this study.

As shown in Fig. 5b, the slurry viscosity decreases with the increase of shear rate, because the colloidal particles belong to a chain-like polymer. When the shear rate increases, each scattered long-chain molecule rotates and shrinks, and the resistance formed by the combination of internal molecules reduces due to structural damage, resulting in a large reduction in viscosity. When the shear rate is between 10~100 s^{-1}, the viscosity decreases rapidly and the shear thinning phenomenon is obvious.

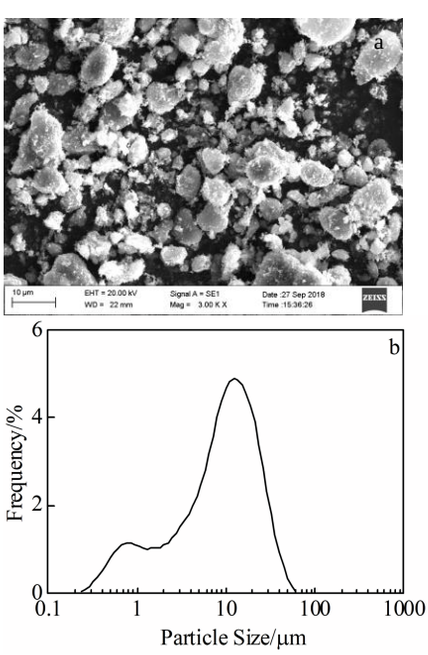

Fig.4 SEM morphology (a) and particle size (b) of TCP powders

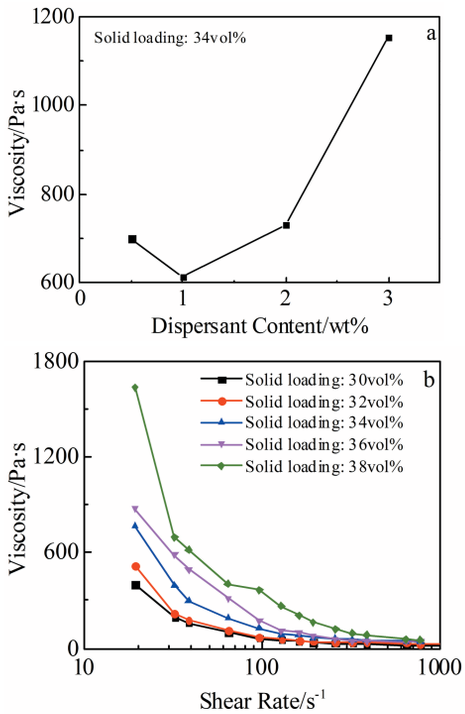

Fig.5 Rheological properties of slurry: (a) viscosity-dispersant content curve; (b) viscosity-shear rate curves with different solid loadings

2.3 Printing parameters

The printing parameters for preparation of porous TCP scaffolds are shown in Table 1. When the printing pressure is 0.3 MPa, the printing speed is the key factor to determine the formability of the scaffolds. Fig. 6 shows the green porous TCP scaffolds printed at different printing speeds. When the printing speed is slow (8 mm/s), the printing wires pile up, which reduces the macroscopic porosity. When the printing speed is fast (13 mm/s), the slurry does not have sufficient time to solidify and the printing wire stretches and even breaks, which affects the scaffold strength. Severe squeezing occurs between the layers, and the shape of the lower part changes, affecting the printing accuracy. Therefore, the optimum print speed in this study is 10 mm/s. At the same time, when the layer height is low, the needle scrapes into the printed layer. The structure of a single print wire is destroyed, which affects the surface morphology and mechanical properties of the scaffolds. When the layer height is high, the printing wire does not closely contact with the printing interface. The printing wire severely deforms, affecting the printing accuracy.

Table 1 Printing parameters for preparation of porous TCP scaffolds

Nozzle diameter/mm	Layer height/mm	Printing speed/mm·s^{-1}	Printing pressure/MPa
0.15	0.13	10	0.3

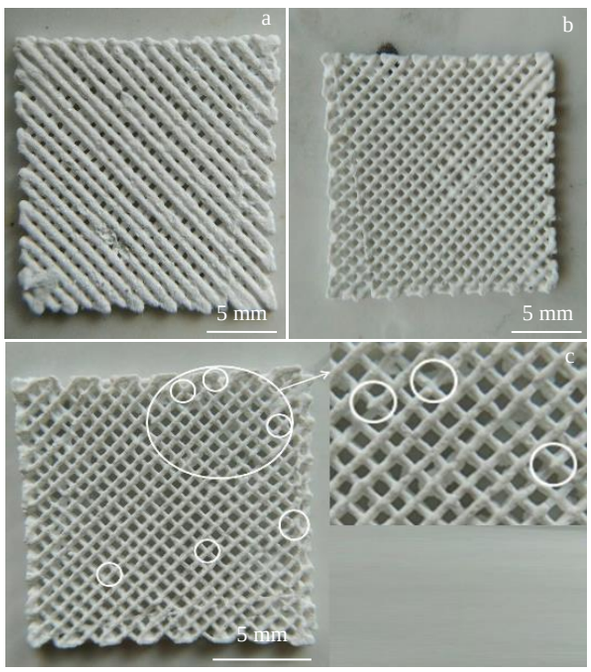

Fig.6 Porous TCP scaffolds printed at different printing speeds: (a) 8 mm/s, (b) 10 mm/s, and (c) 13 mm/s

2.4 Surface morphology of green and sintered TCP scaffolds

Fig. 7 shows the appearances of green and sintered porous TCP scaffolds for implantation tests. The scaffolds show a certain degree of shrinkage after sintering, but they do not crack or deform after sintering. The pore size and pore morphology of scaffolds are uniform, and a certain degree of connectivity still remains. The printed scaffolds have good formability, indicating that it is feasible to print porous TCP scaffolds by 3DGP.

Porous TCP scaffolds prepared by 3DGP are observed by SEM, as shown in Fig. 8. It can be seen that the square pore structure is arranged neatly. The pore diameter is uniform, and the pores are connected with each other. The whole structure of green and sintered scaffolds is intact without obvious defects and cracks. Fig. 8a and 8e show that the printing wire becomes denser after sintering, indicating that sintering can sufficiently diffuse the elements. Fig. 8b and 8f show that the printing line has some micropores due to the decomposition of organic matter during sintering. The width of contact portions of two printing wires before and after sintering is 230±10 and 200±20 μm, respectively. As shown in Fig. 8c and 8g, the size of single printing line before and after sintering is 160±20 and 130±10 μm, respectively. The printing line shows a certain degree of shrinkage. As the temperature increases, the migration of ceramic particles to the surface causes the decrease of surface energy, and the movement of grain boundaries eliminates the pores, resulting in the shrinkage. At the point where the printing wires contact with each other, the width of the printing line is slightly larger due to gravity. Fig. 8h shows that the macroscopic pores of sintered porous TCP scaffolds are square holes with a width of 350±10 μm. In addition, the microscopic pores have different sizes on the surface of scaffolds. This multi-scale pore structure is beneficial to the growth and redistribution of bone cells and new blood vessels. Besides, the densification processes occur after sintering, such as reduction of surface area and porosity, grain boundary formation, grain growth, and improvement of mechanical properties.

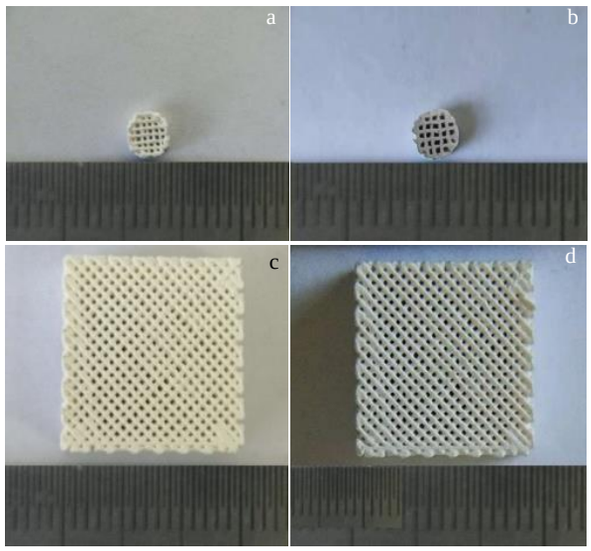

Fig.7 Appearances of green (a, c) and sintered (b, d) porous TCP scaffolds

2.5 Porosity and shrinkage of sintered scaffolds

The prepared TCP scaffolds have a uniform pore structure on the front side. The printing wire contains many micropores, and the side appearance shows a bundle-like arrangement. Fig. 9 shows the surface and side view of sintered porous TCP scaffolds prepared by 3DGP. The average porosity of the scaffolds is tested as 62.1%. In addition, the shrinkage ratio of the scaffolds in all directions is calculated according to Eq.(1):

$$\text{Shrinkage} = \frac{D_0 - D_t}{D_0} \times 100\% \quad (1)$$

where D_0 and D_t are the scaffold sizes before and after sintering, respectively. As shown in Table 2, the shrinkage ratios of the scaffolds in the three directions of length, width, and height caused by sintering are 11.44%±0.20%, 9.41%±0.23%, and 10.57%±0.20%, respectively. The scaffolds shrink uniformly in the three directions, ensuring the integrity of the

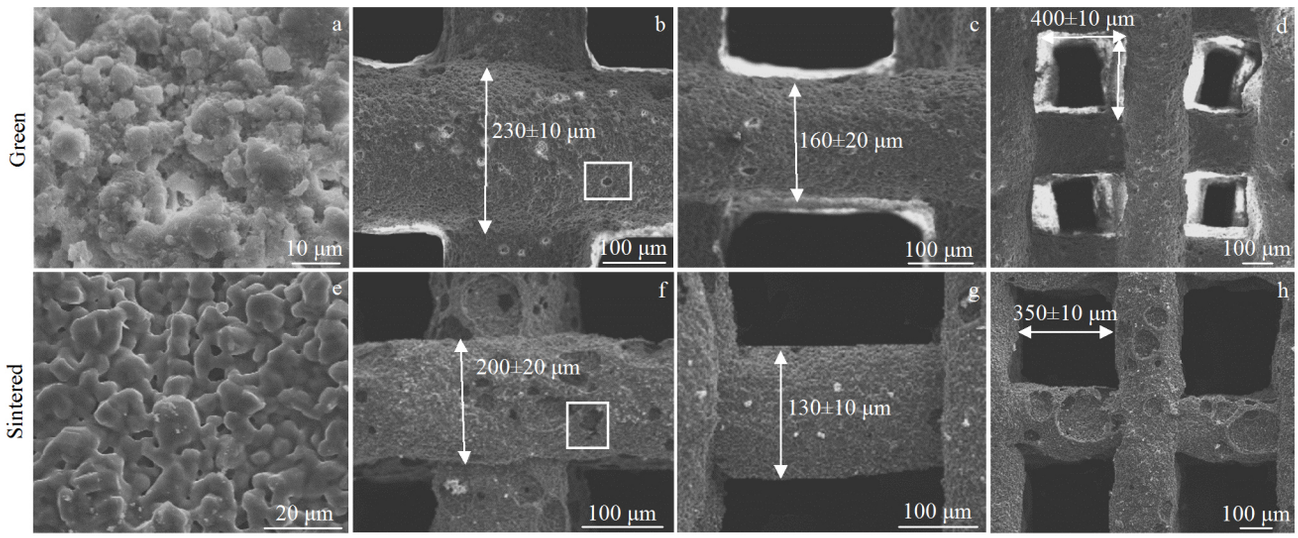

Fig.8 SEM images of green (a~d) and sintered (e~h) porous TCP scaffolds

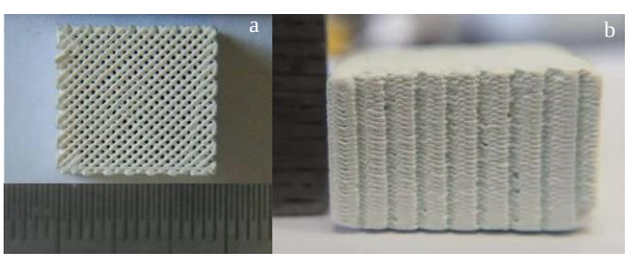

Fig.9 Surface (a) and side (b) appearances of sintered porous TCP scaffolds

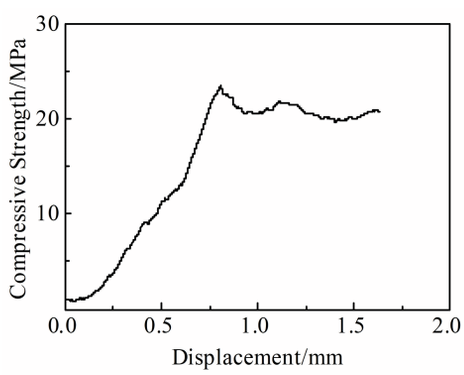

Fig.10 Relationship between compressive strength and TCP scaffold displacement

Table 2 Dimensions of designed model, green, and sintered samples and shrinkage ratio of sintered scaffolds

Dimension	Length	Width	Height
Designed model	15.00 mm	15.00 mm	8.00 mm
Green sample	14.69±0.10 mm	14.45±0.13 mm	7.19±0.13 mm
Sintered sample	13.01±0.23 mm	13.09±0.10 mm	6.43±0.10 mm
Shrinkage ratio	11.44%±0.20%	9.41%±0.23%	10.57%±0.20%

macrostructure before and after sintering.

2.6 Mechanical properties of porous TCP scaffolds

The compressive strength of the scaffolds is related to the aperture and porosity of the scaffolds for the same materials. In the case of the same printing filament, the larger the aperture of the scaffold, the lower the strength. In addition, the mechanical properties of the scaffolds decrease with the increase of porosity. Fig.10 shows the compressive strength of porous TCP scaffolds after sintering at 1150 °C for 2 h. It shows that the average compressive strength is 22.6±0.12 MPa. As shown in Table 3, the compressive strength of natural cancellous bone is generally 0.1~16 MPa[30], and its porosity is 50%~90%[5]. Under the situation that the porosity of the scaffolds is approximately the same, the printed TCP bioscaffolds by 3DGP have higher compressive strength and can better satisfy the requirements of human cancellous bone for the porosity and strength of implanted scaffolds.

Table 3 Properties of TCP scaffolds by different producing processes

Preparation technique	Material	Compressive strength/MPa	Porosity/%
3D printing	TCP	56.7±1.1[27]	-
Freeze-casting	Hydroxyapatite/TCP	5.0±0.1[28]	60
-	Cortical bone	130~180[29]	<10[5]
-	Cancellous bone	0.1~16[30]	50~90[5]
3DGP	TCP	22.6±0.12	62.1±0.10

2.7 X-ray results of implanted scaffolds

Fig. $11a_1$~$11a_3$ show the femoral condyles of rabbits after implantation for 1, 3, and 6 weeks, respectively. Fig. $11a_1$ shows some areas of the scaffold surface are covered by callus

Fig.11 Appearances (a_1~a_3) and X-ray scan results (b_1~b_3) of TCP scaffolds implanted in body for different periods: (a_1, b_1) 1 week, (a_2, b_2) 3 weeks, and (a_3, b_3) 6 weeks

and obvious inflammatory and edematous reactions can be seen. Fig. 11a_2 and 11a_3 show that the entire surface of the scaffolds is covered by the sturdy callus. Fig. 11b_1~11b_3 show the X-ray scan results of the femoral condyles of rabbits after implantation for 1, 3, and 6 weeks, respectively. It is obvious that the scaffolds are stably fixed inside the defect and the overall scaffold structure is clearly visible. There are no inflammatory and edema reactions.

2.8 Histological analysis

Fig. 12 shows the histological image after implantation of TCP scaffold for 4 months. In the center of TCP scaffold, bone cells grow, accompanied by the bone trabecula formation. The porous scaffold fits well with the surrounding bone tissue and no inflammatory cells are found around the porous scaffolds. The results show that porous TCP scaffold has good biocompatibility, which is of great significance for the successful repair of cancellous bone.

In summary, the particle size of TCP powders affects the densification process of printing line during subsequent sintering. The solid loading of the slurry affects the viscosity and fluidity of the slurry during 3DGP process. When the viscosity of the slurry is too low, the curing time of the printing line is long, and the formability of the scaffolds is not good. When the viscosity of the slurry is too high, the fluidity is poor, and the nozzle is easily clogged. Shrinkage is a very important indicator during the sintering process. It is directly related to the dimensional tolerances and yield of ceramic scaffolds. The scaffolds prepared by 3DGP can meet the

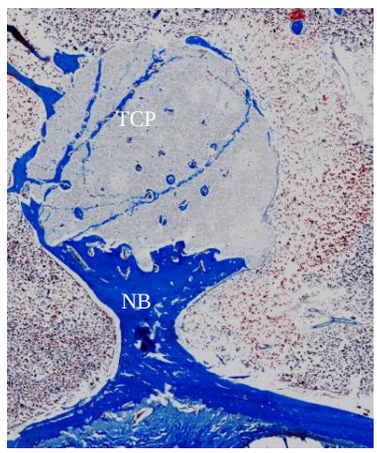

Fig.12 Histological image after 4 months of implantation (NB: newly formed bone)

strength and porosity requirements of cancellous bone. The porous TCP scaffold after implantation into the bone defect site of rabbits shows good biocompatibility.

3 Conclusions

1) Porous tricalcium phosphate (TCP) scaffolds for cancellous bone tissue engineering can be successfully prepared by 3D gel-printing (3DGP) technique in this study. The slurry suitable for 3DGP was prepared using TCP powders with an average particle size of 8.99 μm. The suitable solid loading of the ceramic slurry is 34vol%.

2) The pore size of sintered scaffolds is approximately 350 μm×350 μm, and the shrinkage ratio of scaffolds along three directions of length, width and height after sintering is 11.44%±0.20%, 9.41%±0.23%, 10.57%±0.20%, respectively. The average compressive strength and the porosity of the sintered scaffolds are 22.6±0.12 MPa and 62.1%, respectively, which satisfy the requirements of human cancellous bone. The high porosity is suitable for cell proliferation and nutrient delivery, which is controlled by the slurry and printing parameters.

3) Rabbit femoral defect experiments show that TCP scaffolds printed by 3DGP have good biocompatibility. No inflammation and edema are found after the implantation of scaffold in rabbits for 1, 3 and 6 weeks. The new callus formation is observed around the scaffold, indicating that the TCP scaffolds can be used for repairing cancellous bone tissue engineering.

References

1 Shao Huiping, Yu Xinding, Lin Tao *et al*. *Ceramics International* [J], 2020, 46(9): 13 082

2 Henkel J, Woodruff M A, Epari D R *et al*. *Bone Research*[J], 2013, 1(1): 216

3 Li R, Nauth A, Li C *et al*. *Journal of Orthopaedic Trauma*[J], 2012, 26(12): 689

4 Ekwaro-Osire S, Wanki G, Dias J P. *Journal of Integrated Design and Process Science*[J], 2017, 21(3): 7

5 Bose S, Vahabzadeh S, Bandyopadhyay A. *Materials Today*[J], 2013, 16(12): 496

6 Vazquez-Portalatin N, Kilmer C E, Panitch A *et al*. *Biomacromolecules*[J], 2016, 17(10): 3145

7 Masala S, Nano G, Marcia S *et al*. *Neuroradiology*[J], 2012, 54(11): 1245

8 Shao Huiping, He Jianzhuang, Lin Tao *et al*. *Ceramics International*[J], 2019, 45(1): 1163

9 Pei Xuan, Ma Liang, Zhang Boqing *et al*. *Biofabrication*[J], 2017, 9(4): 45 008

10 Saiz E, Boccaccini A R, Chevalier J *et al*. *Journal of the European Ceramic Society*[J], 2018, 38(3): 821

11 Zhang B, Pei X, Song P *et al*. *Composites Part B: Engineering* [J], 2018, 155: 112

12 Shao Huiping, Zhang Yumeng, Lin Tao *et al*. *Journal of Materials Science*[J], 2020, 55(18): 7870

13 Zhang Boqing, Sun Huan, Wu Lina *et al*. *Bio-Design and Manufacturing*[J], 2019, 2(3): 161

14 Sun Huan, Hu Cheng, Zhou Changchun *et al*. *Materials & Design*[J], 2020, 189: 108 540

15 Bose S, Banerjee D, Shivaram A *et al*. *Materials & Design*[J], 2018, 151: 102

16 Yao Qingqiang, Wei Bo, Guo Yang *et al*. *Journal of Materials Science: Materials in Medicine*[J], 2015, 26(1): 51

17 Kang S W, Bae J H, Park S A *et al*. *Biotechnology Letters*[J], 2012, 34(7): 1375

18 Roopavath U K, Malferrari S, Van Haver A *et al*. *Materials & Design*[J], 2019, 162: 263

19 Kim Y S, Shin Y S, Choi J W *et al*. *Annals of Biomedical Engineering*[J], 2015, 43(9): 2153

20 Park S A, Kim G H, Jeon Y C *et al*. *Journal of Materials Science: Materials in Medicine*[J], 2009, 20(1): 229

21 Li Jinghui, Zhang Lei, Lv Shengyi *et al*. *Journal of Biotechnology*[J], 2011, 151(1): 87

22 Ren Xiangyuan, Shao Huiping, Lin Tao *et al*. *Materials & Design*[J], 2016, 101: 80

23 Zhang Yumeng, Shao Huiping, Lin Tao *et al*. *Ceramic International*[J], 2019, 45(16): 20 493

24 Nie Huali, Zhu Limin. *International Journal of Biological Macromolecules*[J], 2007, 40(3): 261

25 Serra I R, Fradique R, Vallejo M C S *et al*. *Materials Science and Engineering C*[J], 2015, 55: 592

26 Torres A L, Gaspar V M, Serra I R *et al*. *Materials Science and Engineering C*[J], 2013, 33(7): 4460

27 Bose S, Sarkar N, Banerjee D. *Materials Today Chemistry*[J], 2018, 8: 110

28 Macchetta A, Turner I G, Bowen C R. *Acta Biomaterialia*[J], 2009, 5(4): 1319

29 Espalin D, Arcaute K, Rodriguez D *et al*. *Rapid Prototyping Journal*[J], 2010, 16(3): 164

30 Hernandez C J, Beaupre G S, Keller T S *et al*. *Bone*[J], 2001, 29(1): 74

3D凝胶打印制备用于松质骨工程的TCP多孔支架

邵慧萍[1]，俞新鼎[1]，张雨梦[1]，杨思明[2]

(1. 北京科技大学 新材料技术研究院, 北京 100083)

(2. 中国人民解放军总医院 解放军医学院 伤口修复与再生重点实验室, 北京 100853)

摘　要：通过3D凝胶打印（3DGP）技术制备了高强度和高孔隙率的磷酸三钙（TCP）多孔支架，通过扫描电子显微镜（SEM）观察支架的微观形态，并通过初步的动物实验评估了多孔支架的生物相容性。研究结果表明，适合打印的浆料固含量为34%（体积分数），打印支架在长度、宽度和高度方向上的收缩率分别为11.44%±0.20%，9.41%±0.23%和10.57%±0.20%。当支架在1150 ℃下烧结2 h后，支架的抗压强度为22.6±0.12 MPa，孔隙率约为62.1%。初步的动物植入实验显示多孔TCP支架在兔股骨髁缺损处未引起明显的排斥反应，并在骨与支架的连接处未见炎症反应或慢性炎症反应。通过3DGP技术制备的多孔TCP支架具有良好的生物相容性和力学性能，有望满足松质骨的植入要求，为下一步的实验研究打下基础。

关键词：TCP；多孔支架；3DGP；兔子；松质骨

作者简介：邵慧萍，女，1973年生，博士，副教授，北京科技大学新材料技术研究院，北京 100083，E-mail：shaohp@ustb.edu.cn